

*t*-Bu), 2.40 (s, NMe), 2.54 (s, 4NMe<sub>2</sub>), 6.5 (d), 7.35 (d), 6.6-6.9 (m, aromatics); <sup>13</sup>C NMR (C<sub>6</sub>D<sub>6</sub>, 30 °C) δ 242.6 (NMe), 22.7 (NMe), 35.6 (CMe<sub>3</sub>), 31.7 (CMe<sub>3</sub>), 40.1 (NMe<sub>2</sub>). Anal. Calcd for ZrC<sub>48</sub>H<sub>68</sub>N<sub>4</sub>O<sub>2</sub>: C, 69.92; H, 8.33; N, 6.78. Found: C, 69.39; H, 8.65; N, 6.79.

Zr(OAr-2,6-*t*-Bu<sub>2</sub>)<sub>2</sub>[3F-C<sub>6</sub>H<sub>4</sub>NC(CH<sub>3</sub>)=C(CH<sub>3</sub>)NC<sub>6</sub>H<sub>4</sub>-3F] (4)<sup>3F</sup>. <sup>1</sup>H NMR (C<sub>6</sub>D<sub>5</sub>CD<sub>3</sub>, -10 °C) δ 1.14 (s, *t*-Bu), 1.95 (s, NMe), 6.8-7.1 (m, aromatics).

Zr(OAr-2,6-*t*-Bu<sub>2</sub>)<sub>2</sub>[3OMe-C<sub>6</sub>H<sub>4</sub>NC(CH<sub>3</sub>)=C(CH<sub>3</sub>)NC<sub>6</sub>H<sub>4</sub>-3OMe] (4)<sup>3OMe</sup>. <sup>1</sup>H NMR (C<sub>6</sub>D<sub>5</sub>CD<sub>3</sub>, 0 °C) δ 1.19 (s), 1.51 (s, *t*-Bu), 2.09 (s, NMe), 3.37 (s, 3OMe), 6.7-7.4 (m, aromatics).

Zr(OAr-2,6-*t*-Bu<sub>2</sub>)<sub>2</sub>[4OMe-C<sub>6</sub>H<sub>4</sub>NC(CH<sub>3</sub>)=C(CH<sub>3</sub>)NC<sub>6</sub>H<sub>4</sub>-4OMe] (4)<sup>4OMe</sup>. <sup>1</sup>H NMR (C<sub>6</sub>D<sub>5</sub>CD<sub>3</sub>, -5 °C) δ 1.24 (s), 1.58 (s, *t*-Bu), 2.09 (s, NMe), 3.29 (s, 4OMe), 6.8-7.4 (m, aromatics).

Zr(OAr-2,6-*t*-Bu<sub>2</sub>)<sub>2</sub>[4Cl-C<sub>6</sub>H<sub>4</sub>NC(CH<sub>3</sub>)=C(CH<sub>3</sub>)NC<sub>6</sub>H<sub>4</sub>-4Cl] (4)<sup>4Cl</sup>. <sup>1</sup>H NMR (C<sub>6</sub>D<sub>5</sub>CD<sub>3</sub>, 0 °C) δ 1.13 (s), 1.47 (s, *t*-Bu), 1.94 (s, NMe), 6.7-7.3 (m, aromatics).

Zr(OAr-2,6-*t*-Bu<sub>2</sub>)<sub>2</sub>[4NMe<sub>2</sub>-C<sub>6</sub>H<sub>4</sub>NC(CH<sub>3</sub>)=C(CH<sub>3</sub>)NC<sub>6</sub>H<sub>4</sub>-4NMe<sub>2</sub>] (4)<sup>4NMe<sub>2</sub></sup>. <sup>1</sup>H NMR (C<sub>6</sub>D<sub>5</sub>CD<sub>3</sub>, -10 °C) δ 1.29 (s), 1.61 (s, *t*-Bu), 2.10 (s, NMe), 2.50 (s, NMe<sub>2</sub>), 6.9-7.4 (m, aromatics). Anal. Calcd for ZrC<sub>48</sub>H<sub>68</sub>N<sub>4</sub>O<sub>2</sub>: C, 69.92; H, 8.33; N, 6.78. Found: C, 68.82; H, 8.55; N, 6.86.

**Kinetic Measurements.** The rate of intramolecular coupling of the bis(η<sup>2</sup>-iminoacyl) compounds was determined by monitoring the changes in the <sup>1</sup>H NMR spectra on thermolysis in the temperature-controlled probe of an NMR spectrometer. In nearly all cases the extent of reaction

was obtained by integrating the ratio's of the *t*-Bu or *i*-Pr resonances of the aryloxy ligands in the starting material and enediamide product. In one case, 3<sup>2,6Me<sub>2</sub></sup>, thermolysis was carried out by total immersion of the sealed 5-mm <sup>1</sup>H NMR tube into a constant temperature oil bath. The sample was then rapidly cooled at various times, and the extent of reaction was determined by <sup>1</sup>H NMR. Both the rate constants and activation parameters were determined with the use of a linear least-squares fitting procedure.

**Acknowledgment.** We thank the Department of Energy (Pittsburgh Energy Technology Center; Grant DE-FG 22-85PC80909) and the National Science Foundation (Grant CHE-8612063) for support of this research. I.P.R. gratefully acknowledges the Camille and Henry Dreyfus Foundation for the award of a Teacher-Scholar Grant and the Alfred P. Sloan Foundation for the award of a Fellowship. L.D.D. gratefully acknowledges Amoco Corporation for an Industrial Fellowship.

**Registry No.** 1a, 110316-44-4; 1b, 110316-45-5; 2a, 110316-36-4; 2b, 110316-37-5; 3<sup>H</sup>, 105899-83-0; 3<sup>3F</sup>, 112320-06-6; 3<sup>3OMe</sup>, 112320-07-7; 3<sup>4OMe</sup>, 112320-08-8; 3<sup>4Cl</sup>, 112320-09-9; 3<sup>4NMe<sub>2</sub></sup>, 112320-10-2; 3<sup>2,6Me<sub>2</sub></sup>, 98065-02-2; 3a, 110316-46-6; 4<sup>H</sup>, 110316-40-0; 4<sup>3F</sup>, 112347-47-4; 4<sup>3OMe</sup>, 112347-48-5; 4<sup>4OMe</sup>, 112347-49-6; 4<sup>4Cl</sup>, 112347-50-9; 4<sup>4NMe<sub>2</sub></sup>, 112347-51-0; 4<sup>2,6Me<sub>2</sub></sup>, 110316-38-6; 4a, 110316-39-7; 5<sup>H</sup>, 105899-84-1; 6<sup>H</sup>, 110316-41-1.

## Topological Kinetic Effects: Complexation of Interlocked Macrocyclic Ligands by Cationic Species

Anne-Marie Albrecht-Gary,\*<sup>†</sup> Christiane Dietrich-Buchecker,<sup>†</sup> Zeinab Saad,<sup>†</sup> and Jean-Pierre Sauvage\*<sup>†</sup>

Contribution from the Laboratoire de Chimie Physique et d'Electroanalyse, UA au CNRS 405, EHICS, 67000 Strasbourg, France, and the Laboratoire de Chimie Organo-Minérale, UA au CNRS 422, Institut de Chimie, 1, rue Blaise Pascal, 67000 Strasbourg, France.

Received June 15, 1987

**Abstract:** Complexation kinetic studies of various metal cations by a catenand have been performed. For comparison, the properties of some related open chain or monocyclic ligands have also been examined. Copper(I) and silver(I) catenane formation obeys a classical second-order rate law. The same is true for the model ligands examined, m-30 and dap. For Cu(dap)<sub>2</sub><sup>+</sup>, the rate-limiting step corresponds to the formation of the bis-chelate complex from the monochelated one. On the other hand, Li<sup>+</sup>, Cd<sup>2+</sup>, Zn<sup>2+</sup>, and Co<sup>2+</sup> catenates are formed in two distinct steps. The first process is second order, and it is likely to be the binding of the metallic cation to one of the chelating subunits. The second step is more intriguing. It does not depend on the metal concentration, and it might correspond to the gliding motion of one ring within the other while the second chelate fragment attempts to coordinate to the metal center.

The fascinating properties of topologically novel molecules have been considered by several groups in the past. Interlocked rings were discussed several years ago, and synthetic approaches have now been developed.<sup>1-5</sup> In recent years a molecular Möbius strip has also been obtained as well as its cylindrical topological isomer.<sup>6,7</sup> Closed knotted cycles have also been envisaged,<sup>2,3,8</sup> although the preparation of such systems is still a challenge to synthetic chemists. [2]-Catenands consist of two interlocked macrocyclic ligands, and the first members of this new class of molecules have recently been reported.<sup>9,10</sup> The ligands are obtained by demetalation of their corresponding complexes, the catenates, the latter being synthesized from open chain ligands complexed to a transition-metal center (copper(I)) used as templating moiety.

Catenands represent a unique example of molecules displaying both topological novelty and the ability to interact with transition

metals or other cationic species. In the complexation-decomplexation process the molecular system undergoes a complete rearrangement, which leads to drastic changes in shape (topography). However, since no covalent bond is cleaved within the catenand, the bond connectivity is obviously retained (topology)

(1) Wasserman, E. *J. Am. Chem. Soc.* **1960**, *82*, 4433.

(2) Frisch, H. L.; Wasserman, E. *J. Am. Chem. Soc.* **1961**, *83*, 3789.

(3) Schill, G. In *Catenanes, Rotaxanes and Knots*; Academic: New York, 1971.

(4) Harrison, I. T. *J. Chem. Soc., Perkin Trans 1* **1974**, 301.

(5) Agam, G.; Graiver, D.; Zilkha, A. *J. Am. Chem. Soc.* **1976**, *98*, 5214.

(6) Walba, D. M.; Richards, R. M.; Haltiwanger, R. C. *J. Am. Chem. Soc.* **1982**, *104*, 3219.

(7) (a) Walba, D. M. In *Chemical Applications of Topology and Graph Theory*; King, R. B., Ed.; Elsevier: New York, 1983. (b) Walba, D. M. *Tetrahedron* **1985**, *41*, 3161.

(8) Walba, D. M.; Armstrong, J. D., III; Perry, A. E.; Richards, R. M.; Homan, T. C.; Haltiwanger, R. C. *Tetrahedron* **1986**, *42*, 1883.

(9) Dietrich-Buchecker, C. O.; Sauvage, J.-P.; Kintzinger, J.-P. *Tetrahedron Lett.* **1983**, *46*, 5095.

(10) Dietrich-Buchecker, C. O.; Sauvage, J.-P.; Kern, J.-M. *J. Am. Chem. Soc.* **1984**, *106*, 3043.

\*Laboratoire de Chimie Physique et d'Electroanalyse.

†Laboratoire de Chimie Organo-Minérale.

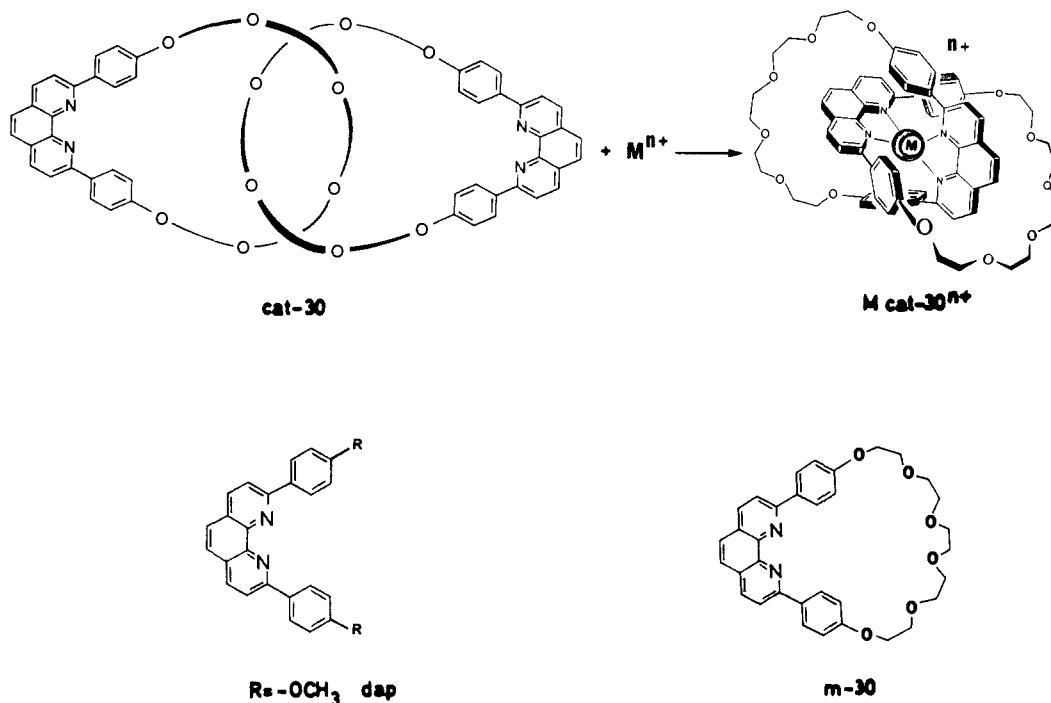


**Figure 1.** Topographical change during the overall formation reaction of a catenate and the structure of ligands related to the catenand, dap(2,9-dianisyl-1,10-phenanthroline) and m-30 (macrocyclic phenanthroline).

in the course of the metalation–demetalation reactions, implying that the *topological properties* of the molecule are not affected. This effect was clearly shown by X-ray structural studies performed on a [2]-catenand<sup>11</sup> and its corresponding complexes, a copper(I)<sup>11</sup> or a proton catenate.<sup>12</sup> In the complexes, the two 2,9-diphenyl-1,10-phenanthroline (dpp) subunits are really entwined by coordination to the central species, whereas in the ligand the two dpp fragments are a long distance apart. A gliding motion of one ring within the other converts one form into the other in a completely reversible process.

We have recently shown that copper(I) catenates are kinetically very stable and that, in particular, the gliding motion of both rings required in order to demetalate is a very slow process.<sup>13</sup> Catenates are thus much less labile than their open chain analogues, although the topography (shape) of both complexes around the metal is almost identical. This effect should obviously be highly dependent on the ring size, but in the present article only the bis-30-membered-ring catenand will be considered. We now report a kinetic study of the reverse reaction: formation of a catenate from the free ligand and a given species. This study was undertaken mainly to answer the following intriguing question: will a catenand act as a single molecule or will it behave as a set of two separate coordinated rings? Clearly, in the overall coordination process, X-ray and NMR studies have demonstrated that a catenand can be considered as a single ligand. However, fine kinetic analysis of the complexation process shows several steps in a few examples. This strongly suggests that the two dpp subunits act as separate ligands at the very beginning of the coordination reaction, further evolution of the system being governed by the interaction between the two interlocked rings and their dpp fragments.

The overall reaction studied is represented in Figure 1. The catenand studied cat-30 contains two 30-membered interlocked rings and the cationic species considered are copper(I), cobalt(II), silver(I), lithium(I), zinc(II), and cadmium(II). In order to compare the interlocked macrocyclic system to mono- or acyclic ligands, the isolated constitutive ring m-30 and the open chain

chelate dap have also been examined.

#### Experimental Section

**Materials.** 2,9-Dianisyl-1,10-phenanthroline (dap),<sup>14</sup> the macrocyclic ligand m-30,<sup>14</sup> and the catenand cat-30<sup>10</sup> were synthesized as previously published.

$[\text{Cu}(\text{CH}_3\text{CN})_4] \cdot [\text{BF}_4]$  was prepared by the literature method.<sup>15</sup> The commercial salts  $\text{LiClO}_4 \cdot 3\text{H}_2\text{O}$  (Merck, p.a.) and  $\text{M}(\text{ClO}_4)_2 \cdot 6\text{H}_2\text{O}$  [ $\text{M} = \text{Co}(\text{II})$  (Fluka, p.a.),  $\text{M} = \text{Zn}(\text{II})$  and  $\text{Cd}(\text{II})$  (Alfa-Ventron, p.a.)] were used without further purification. Silver(I) solutions [ $\text{AgClO}_4 \cdot \text{H}_2\text{O}$  (Fluka, p.a.)] were protected from light. Solutions of very hygroscopic salts [ $\text{Co}(\text{II})$ ,  $\text{Zn}(\text{II})$ , and  $\text{Cd}(\text{II})$ ] were titrated with EDTA by classical methods. Lithium(I) and silver(I) solutions were prepared by accurate weighing.

The solvent selected for this work was the mixed solvent acetonitrile:methylene chloride:water (80:10:10 v/v). This solvent dissolved the free catenand up to about  $2 \times 10^{-4}$  mol  $\text{L}^{-1}$  and the metal salts up to about  $10^{-1}$  mol  $\text{L}^{-1}$ .  $\text{CH}_3\text{CN}$  and  $\text{CH}_2\text{Cl}_2$  were commercial grade solvents from Merck (Uvasol).

The ionic strength was adjusted to 0.1 with tetrabutylammonium perchlorate (Fluka, purum). The latter was recrystallized<sup>16</sup> twice.

Special care was taken for the experiments with  $[\text{Cu}(\text{CH}_3\text{CN})_4] \cdot [\text{BF}_4]$ . All the solutions were made in a glovebox (Jaram) with deaerated solvents. Gas-tight syringes (Hamilton) were used for sampling and injecting the reactants in the stopped-flow system. Teflon syringe needles (Hamilton) were used in order to prevent metallic contamination.

**Preliminary Spectrophotometric Determinations and Kinetic Measurements.** A fast mixing device was necessary for measuring the formation rates of the various complexes so spectrophotometric detection was used (stopped-flow spectrophotometer Durrum-Gibson D-110). The kinetic data were recorded on a Datalab transient recorder and treated on-line with an Apple II microcomputer and a first-order kinetics program.<sup>17</sup>

The preliminary spectrophotometric study of the ligands and of the corresponding complexes formed was carried out with a Cary 17 spectrophotometer. The electronic spectra obtained are presented in Figure 2. The arrows indicate the wavelength chosen for the kinetic measurements.

A typical experimental recording is presented in Figure 3a. It corresponds to an exponential signal. In the presence of metal salt in excess, the rate law found is first order with respect to the ligand. If variable

(11) Cesario, M.; Dietrich-Buchecker, C. O.; Guilhem, J.; Pascard, C.; Sauvage, J.-P. *Chem. Commun.* **1985**, 244.

(12) Cesario, M.; Dietrich-Buchecker, C. O.; Edel, A.; Guilhem, J.; Kintzinger, J.-P.; Pascard, C.; Sauvage, J.-P. *J. Am. Chem. Soc.* **1986**, *108*, 6250.

(13) Albrecht-Gary, A.-M.; Saad, Z.; Dietrich-Buchecker, C. O.; Sauvage, J.-P. *J. Am. Chem. Soc.* **1985**, *107*, 3205.

(14) Dietrich-Buchecker, C. O.; Sauvage, J. P. *Tetrahedron Lett.* **1983**, *24*, 5091.

(15) Meerwein, H.; Hederich, V.; Wunderlich, K. *Ber. Dtsch. Pharm. Ges.* **1958**, *63*, 548.

(16) House, M. O.; Feng, E.; Peet, N. P. *J. Org. Chem.* **1971**, *36*, 2371.

(17) Lagrange, J.; Lagrange, P. *J. Chim. Phys.* **1984**, *81*, 425.

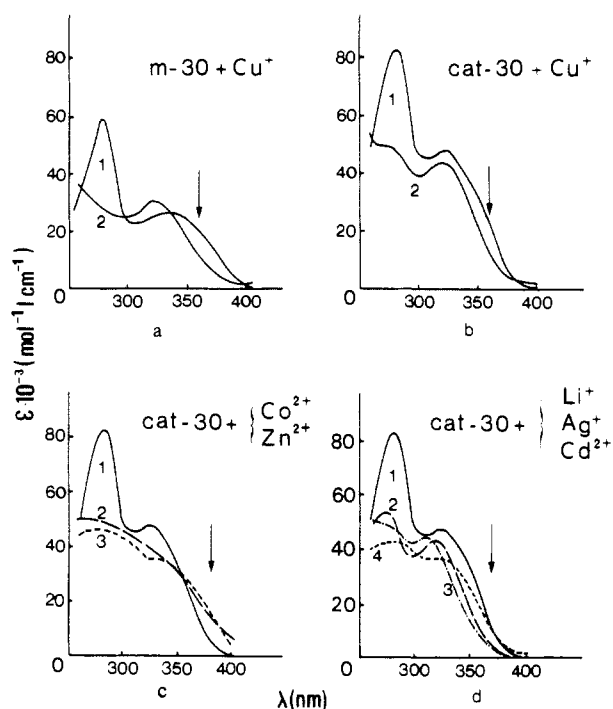


**Figure 2.** Electronic spectra of ligands and corresponding complexes. Solvent:  $\text{CH}_3\text{CN}:\text{CH}_2\text{Cl}_2:\text{H}_2\text{O}$  (80:10:10 v/v);  $I = 0.1$ ,  $T = (25.0 \pm 0.1)^\circ\text{C}$ . (a) 1, m-30; 2,  $\text{Cu}(\text{m-30})^+$ . (b) 1, cat-30; 2,  $\text{Cu}(\text{cat-30})^+$ . (c) 1, cat-30; 2,  $\text{Co}(\text{cat-30})^{2+}$ ; 3,  $\text{Zn}(\text{cat-30})^{2+}$ . (d) 1, cat-30; 2,  $\text{Li}(\text{cat-30})^+$ ; 3,  $\text{Ag}(\text{cat-30})^+$ ; 4,  $\text{Cd}(\text{cat-30})^{2+}$ .

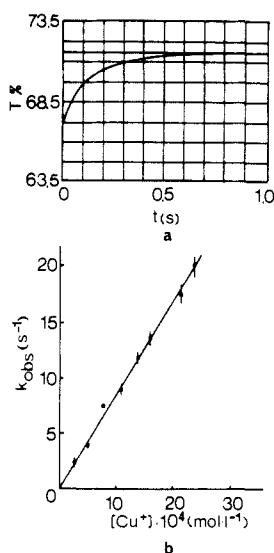


**Figure 3.** (a) Stopped-flow experimental curve obtained for the formation of  $\text{Cu}(\text{cat-30})^+$ ;  $[\text{Cu}(\text{I})]_0 = 7.91 \times 10^{-4} \text{ mol L}^{-1}$ . (b) Variation of the experimental rate constants with the concentration of copper(I) in excess.  $\lambda = 360 \text{ nm}$ ; solvent  $\text{CH}_3\text{CN}:\text{CH}_2\text{Cl}_2:\text{H}_2\text{O}$  (80:10:10 v/v);  $[\text{Cat-30}]_0 = 6 \times 10^{-6} \text{ mol L}^{-1}$ ;  $I = 0.1$ ;  $T = (25.0 \pm 0.1)^\circ\text{C}$ .

amounts of metal salt are used, a first-order rate law with respect to the metal cation is observed, as shown in Figure 3b.

## Results and Discussion

Although m-30 and cat-30 have cyclic structures, the coordinating fragment is simply a dpp chelate. In other words, the ligands discussed in the present article do not strictly belong to the class of molecules studied previously that lead to the so-called *macrocyclic effect*. Usually, macrocyclic ligands lead to extremely slow processes both for metal complex formation and for decomplexation with respect to their open chain analogues. For instance, a 14-membered ring was shown to coordinate to  $\text{Cu}^{2+}$  ca.  $10^4$  times slower than the acyclic compound, but the complex obtained was shown to be ca.  $10^7$  times more inert.<sup>18,19</sup> The effect is partly

**Table I.** Formation Rate Constants  $k_f$  of Copper(I) and Silver(I) Complexes<sup>a</sup>

reaction studied	$k_f$ , $\text{mol}^{-1} \text{L s}^{-1}$
$\text{Cu}(\text{phen})^+ + \text{phen} \xrightarrow{(\text{in H}_2\text{O})} \text{Cu}(\text{phen})_2^+$	$6.2 \times 10^4$ <sup>b</sup>
$\text{Cu}(\text{dap})^+ + \text{dap} \xrightarrow{k_f} \text{Cu}(\text{dap})_2^+$	$(9.2 \pm 0.8) \times 10^5$
$\text{Cu}^+ + \text{m-30} \rightarrow \text{Cu}(\text{m-30})^+$	$\geq 10^7$
$\text{Cu}^+ + \text{cat-30} \rightarrow \text{Cu}(\text{cat-30})^+$	$(8.5 \pm 0.1) \times 10^3$
$\text{Ag}^+ + \text{cat-30} \rightarrow \text{Ag}(\text{cat-30})^+$	$(1.9 \pm 0.1) \times 10^5$

<sup>a</sup> In  $\text{CH}_3\text{CN}:\text{CH}_2\text{Cl}_2:\text{H}_2\text{O}$  (80:10:10 v/v) at  $25^\circ\text{C}$ . <sup>b</sup> Hodges, H. L.; Araujo, M. A. *Inorg. Chem.* **1982**, *21*, 3236.

due to the large number of coordination sites (NH or water molecule) interacting with the transition metal. This situation is drastically different in the case of m-30 and cat-30. The latter molecules contain bidentate chelating sites that can clearly act separately. The cyclic ligand cat-30 might thus be considered as a doubly chelating species whose kinetic properties are extremely different from classical macrocyclic systems, although the overall kinetic inertness of complexes of cat-30 is reminiscent of more classical macrocyclic systems.

**1. Formation Kinetics of Copper(I) Complexes.** The kinetic data for the various copper(I) complexes studied are collected in Table I. The formation reaction of  $\text{Cu}(\text{m-30})^+$  was studied in  $\text{CH}_3\text{CN}:\text{CH}_2\text{Cl}_2:\text{H}_2\text{O}$  (80:10:10 v/v) with a stopped-flow spectrophotometer at a wavelength of 360 nm (Figure 2a). This reaction was too fast for the technique used, and even with a 1:1 stoichiometry ( $[\text{Cu}^+]_0 = 5 \times 10^{-6} \text{ mol L}^{-1}$ ) only the end of the complexation reaction could be observed. Indeed, electronic spectra measurements show that there is no doubt about complete formation of the  $\text{Cu}(\text{m-30})^+$  complex under the experimental conditions used.

The formation of  $\text{Cu}(\text{dap})_2^+$  turned out to be much slower than that of  $\text{Cu}(\text{m-30})^+$ . This reaction was studied under experimental conditions analogous to those used for  $\text{Cu}(\text{m-30})^+$ , at 440 nm.<sup>13,16</sup>

Due to fast complex formation, a 2dap:1Cu<sup>I</sup> stoichiometry was required over a relatively broad concentration range ( $[\text{dap}]_0 = 5 \times 10^{-5}$  to  $5 \times 10^{-4} \text{ mol L}^{-1}$ ). The following rate law was found:

$$v = \frac{d[\text{Cu}(\text{dap})_2^+]}{dt} = k_f[\text{Cu}^+][\text{dap}] \quad (1)$$

with  $k_f$  = second-order rate constant =  $(9.2 \pm 0.8) \times 10^5 \text{ mol}^{-1} \text{L s}^{-1}$ . At first glance, it seems paradoxical that the formation of the open chain complex  $\text{Cu}(\text{dap})_2^+$  is at least one order of magnitude slower than that of the cyclic complex  $\text{Cu}(\text{m-30})^+$ .

Clearly, no macrocyclic effect is found as far as m-30 is concerned. This is due to the bidentate nature of this ring, allowing the coordinated transition metal to keep solvent molecules within its coordination sphere. The function of the pentaoxyethylene fragment of m-30 is only to prevent two such ligands from binding to the same metal center. On the other hand, the situation with dap as a chelate is dramatically different. The formation of the first chelated species  $\text{Cu}(\text{dap})^+$ , supposedly identical with  $\text{Cu}(\text{m-30})^+$ , is likely to be very fast. However, with the acyclic ligand dap, entwining of a second chelate with the first dap molecule is allowed. This step, requiring complete desolvation of the copper(I) atom, is rate-limiting. Such an observation is in good agreement with previous studies on the copper(I) complexes of 1,10-phenanthroline.<sup>21</sup> In this latter case, complexation of the second ligand was found to be slower than that of the first one. Quantitative data are given in Table I. The overall complexation process of  $\text{Cu}^{\text{I}}$  by dap can be expressed by the following equation:

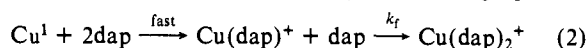


Figure 1 shows schematically the reaction of a catenand with copper(I) to form a catenate.<sup>11,12</sup> There is a large change in

(18) Cabiness, D. K.; Margerum, D. W. *J. Am. Chem. Soc.* **1970**, *92*, 2151.

(19) Busch, D. H. *Acc. Chem. Res.* **1978**, *11*, 392 and references therein.

(20) Edel, A.; Marnot, P. A.; Sauvage, J.-P. *Nouv. J. Chim.* **1984**, *8*, 495.

(21) Hodges, H. L.; de Araujo, M. A. *Inorg. Chem.* **1982**, *21*, 3236.

topography during the reaction, and this prompted us to elucidate its reaction pathway by kinetic measurements. The formation reaction of  $\text{Cu}(\text{cat-30})^+$  was monitored at 360 nm as shown in Figure 2b, with an excess of  $\text{Cu}^I$  with respect to cat-30 ( $[\text{cat-30}]_0 \sim 10^{-5} \text{ mol L}^{-1}$ ). The experimental data obtained are shown in Figure 3.

The following rate law was found:

$$v = \frac{d[\text{Cu}(\text{cat-30})^+]}{dt} = k_f[\text{cat-30}][\text{Cu}^I] \quad (3)$$

$k_f$  = second-order formation rate constant =  $(8.5 \pm 0.1) \times 10^3 \text{ mol}^{-1} \text{ L s}^{-1}$ . Monitoring the catenate formation reaction at a longer wavelength (400 nm) does not modify significantly the rate constant value.

Interestingly, the catenand acts as a single ligand, contrary to dap. In other words, only one step is observed and no intermediate states can be detected, in spite of the highly rigid and organized nature of the final state. This indicates that the entwined topography of the molecule is highly stabilized with respect to all the other possible situations.

The catenand effect might be estimated by comparing the  $k_f$  values for  $\text{Cu}(\text{dap})_2^+$  and  $\text{Cu}(\text{cat-30})^+$ . The formation of the catenate is roughly two orders of magnitude slower than that of its acyclic analogue. On the other hand, our previous kinetic study had shown that the difference was slightly more pronounced as far as the dissociation reaction is concerned. In  $\text{CH}_3\text{CN}/\text{H}_2\text{O}$  (90/10 v/v), the catenate was found to be  $10^3$  times more inert than  $\text{Cu}(\text{dap})_2^+$ . The steric hindrance due to the pentaoxyethylene links may account for the larger inertness of cat-30 to metalation with respect to dap. Those links may interact with the  $\text{Cu}^I$  solvation-desolvation processes and slow down conformational changes of the ligand. In the course of the catenate formation, the second dpp chelate which coordinates to  $\text{Cu}^I$  has to entwine with the first bound dpp fragment. During this motion, it feels the constraint of the pentaoxyethylene link borne by the first dpp. The more rigid and compact situation of the final product  $\text{Cu}(\text{cat-30})^+$  with respect to  $\text{Cu}(\text{dap})_2^+$  may account for the slowing down of the metalation process in the former.

The formation kinetics of other complexes of cat-30 will be discussed below. As the simple rate law found for  $\text{Cu}(\text{cat-30})^+$  appeared intriguing, the study of the other catenates was expected to shine light on the formation reaction pathway and to help elucidate the structure of the intermediate states during transformation of the starting ligand cat-30 to its complexes.

The formation study of the other catenates was performed under experimental conditions very close to those used for  $\text{Cu}(\text{cat-30})^+$ , in the same ternary solvent mixtures  $\text{CH}_3\text{CN}:\text{CH}_2\text{Cl}_2:\text{H}_2\text{O}$  (80:10:10 v/v), with a large excess of metal salt (at least tenfold).

**2. Formation Kinetics of Silver(I) Catenate.** The formation reaction was monitored at 360 nm over a tenfold concentration range of  $\text{Ag}^I$  ( $[\text{Cat-30}]_0 = 5 \times 10^{-6} \text{ mol L}^{-1}$ ;  $[\text{Ag}^I]_0 = 6 \times 10^{-5}$  to  $5 \times 10^{-4} \text{ mol L}^{-1}$ ). The rate law obtained shows a first-order dependence of cat-30:

$$v = \frac{d[\text{Ag}(\text{cat-30})^+]}{dt} = k_{\text{obsd}}[\text{cat-30}] \quad (4)$$

Upon varying the silver(I) concentration, we obtained a linear plot for  $k_{\text{obsd}}$  as a function of  $[\text{Ag}^I]$ , leading to a similar rate law as that found for  $\text{Cu}(\text{cat-30})^+$ :

$$v = \frac{d[\text{Ag}(\text{cat-30})^+]}{dt} = k_f[\text{cat-30}][\text{Ag}^I] \quad (5)$$

$k_f$  = second-order formation rate constant =  $1.9 \times 10^5 \text{ mol}^{-1} \text{ L s}^{-1}$ . The silver catenate formation reaction is 20 times faster than that of its copper(I) analogue. This is not surprising if one considers the respective acetonitrile complexes of these two monovalent cations. Indeed, the copper(I) complex is more stable than the silver(I) complex<sup>22</sup> which might lead to a faster desol-

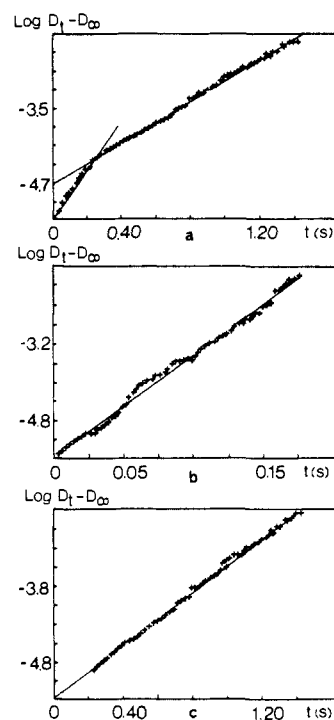


**Figure 4.** Numerical on-line treatment of the kinetic data for the formation reaction of  $\text{Li}(\text{cat-30})^+$ : (a) two first-order rate-limiting steps; (b) separation of the faster one; (c) separation of the slower one.

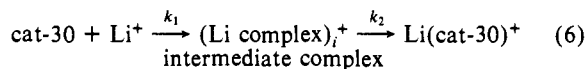
vation reaction for the latter as compared to  $\text{Cu}^I$ .

Among the various species studied,  $\text{Cu}^I$  and  $\text{Ag}^I$  turned out to be the sole cations to form catenates in a one-step reaction. This intriguing observation is likely to be related to the preferred coordination geometry of these cations. Indeed, due to the  $d^{10}$  electronic configuration of  $\text{Cu}^I$  and  $\text{Ag}^I$ , tetrahedral or distorted tetrahedral geometries are expected to be stabilized with respect to higher coordination numbers.<sup>23</sup> Since cat-30 is ideally suited to pseudotetrahedral coordination,<sup>11,12</sup> the good agreement between the favored geometries of both the complexed series and the organic ligand might explain the straightforward formation of the corresponding catenate.

**3. Formation Kinetics of  $\text{Li}^+$ ,  $\text{Zn}^{2+}$ ,  $\text{Cd}^{2+}$ , and  $\text{Co}^{2+}$  Catenates.** The formation reactions of a large number of transition-metal and other cationic catenates have been studied. However, some still unclear processes exist. They may be related to redox reactions, and they have made some results difficult to reproduce, in particular for  $\text{Cu}^{2+}$  and  $\text{Ni}^{2+}$ . On the other hand, the data discussed below have been obtained under strictly controlled experimental conditions and have been repeated several times.

The catenate formation was monitored at 360 nm for  $\text{Li}^+$ , 380 nm for  $\text{Zn}^{2+}$ , 355 nm for  $\text{Cd}^{2+}$ , and 380 nm for  $\text{Co}^{2+}$  in  $\text{CH}_3\text{CN}:\text{CH}_2\text{Cl}_2:\text{H}_2\text{O}$  (80:10:10 v/v) with a stopped-flow spectrophotometer. In all cases,  $[\text{cat-30}] = 6 \times 10^{-6} \text{ mol L}^{-1}$ , and the metal salt (perchlorates) was used over a broad concentration range ( $6 \times 10^{-5}$  to  $9 \times 10^{-4} \text{ mol L}^{-1}$ ). Two rate-limiting steps are found for the four catenates considered, as shown in Figure 4a.

The first exponential signal (Figure 4b) depends linearly on the cation concentration, the latter being present in excess. By contrast, the second exponential signal (Figure 4c) is not affected by the cation concentration. Typical results for  $\text{Li}^+$  complexation are given in Table II. In order to explain these kinetic data, it might be proposed that an intermediate complex is formed in a fast reaction followed by a slow unimolecular rearrangement:



(22) Manahan, S. E.; Iwamoto, R. T. *J. Electroanal. Chem.* **1967**, *14*, 213.

(23) Cotton, F. A.; Wilkinson, G. In *Advanced Inorganic Chemistry*; Wiley: New York, 1972.

**Table II.** Experimental First-Order Rate Constants for the Two Formation Steps of the Catenate  $\text{Li}(\text{cat-30})^+$ <sup>a</sup>

$[\text{Li}^+]_0 \times 10^4$ (mol L <sup>-1</sup> )	fast step $k_{\text{obsd}} \pm 2\sigma$ (s <sup>-1</sup> )	slow step $k'_{\text{obsd}} \pm 2\sigma$ (s <sup>-1</sup> )
0.65	10.3 ± 0.3	1.68 ± 0.02
1.09	18.4 ± 0.5	1.56 ± 0.05
1.63	26.2 ± 0.1	1.74 ± 0.07
2.18	39.5 ± 0.4	1.87 ± 0.15
3.27	51.6 ± 0.8	1.90 ± 0.06
4.08	67.5 ± 1.1	1.20 ± 0.07

<sup>a</sup>Solvent:  $\text{CH}_3\text{CN}:\text{CH}_2\text{Cl}_2:\text{H}_2\text{O}$  (80:10:10 v/v);  $I = 0.1$ ;  $T = 25.0 \pm 0.1$  °C;  $\lambda = 360$  nm;  $[\text{cat-30}]_0 = 6 \times 10^{-6}$  mol L<sup>-1</sup>.

**Table III.** Kinetic Parameters for the Formation of Various Catenates  $\text{M}(\text{cat-30})^{n+}$ <sup>a</sup>

cations	fast step $k_1$ (mol <sup>-1</sup> L s <sup>-1</sup> )	slow step $k_2$ (s <sup>-1</sup> )	desolvation kinetics <sup>b</sup> $k_{\text{H}_2\text{O}}$ (s <sup>-1</sup> )
$\text{Li}^+$	$(1.67 \pm 0.03) \times 10^5$	$1.7 \pm 0.5$	$6 \times 10^8$
$\text{Cd}^{2+}$	$(6.2 \pm 0.07) \times 10^4$	$(1.8 \pm 0.5) \times 10^{-1}$	$2 \times 10^8$
$\text{Zn}^{2+}$	$(9.3 \pm 0.2) \times 10^4$	$(3 \pm 1) \times 10^{-2}$	$3 \times 10^7$
$\text{Co}^{2+}$	$(3.4 \pm 0.1) \times 10^4$	$(6 \pm 2) \times 10^{-3}$	$3 \times 10^5$

<sup>a</sup>Solvent:  $\text{CH}_3\text{CN}:\text{CH}_2\text{Cl}_2:\text{H}_2\text{O}$  (80:10:10 v/v);  $I = 0.1$ ;  $T = 25.0 \pm 0.1$  °C. <sup>b</sup>Reference 28.

The kinetic equations commensurate with the proposed mechanism 6 are as follows:

$$-\frac{d[\text{cat-30}]}{dt} = k_1[\text{Li}^+][\text{cat-30}] \quad (7)$$

$$k_1 = \frac{\bar{k}_{\text{obsd}}}{[\text{Li}^+]}; \text{ second-order rate constant (mol}^{-1} \text{ L s}^{-1}\text{)}$$

$$\frac{d[\text{Li}(\text{cat-30})^+]}{dt} = k_2[(\text{Li complex})_i^+] \quad (8)$$

$$k_2 = \bar{k}'_{\text{obsd}}; \text{ first-order rate constant (s}^{-1}\text{)}$$

$$\text{and } \frac{d[(\text{Li complex})_i^+]}{dt} = k_1[\text{Li}^+][\text{cat-30}] - k_2[(\text{Li complex})_i^+]$$

Similar rate laws and kinetic equations have been obtained for  $\text{Zn}^{2+}$ ,  $\text{Cd}^{2+}$ , and  $\text{Co}^{2+}$  catenates. The respective kinetic parameters are presented in Table III.

**4. Formation of Catenates: Reaction Pathway.** It is noteworthy that the cationic species leading to a two-step complexation reaction have a higher normal coordination number than 4, in contrast to  $\text{Cu}^1$  and  $\text{Ag}^1$ .  $\text{Zn}^{2+}$ ,  $\text{Cd}^{2+}$ , and  $\text{Co}^{2+}$  have been shown to form tris-chelate complexes with unsubstituted 1,10-phenanthroline.<sup>24</sup> From the drastically different behavior of  $\text{Cu}^1$  and  $\text{Ag}^1$  on the one hand and  $\text{Li}^+$ ,  $\text{Zn}^{2+}$ ,  $\text{Cd}^{2+}$ , and  $\text{Co}^{2+}$  on the other hand, we propose the following reaction pathways, schematized in Figure 5.

For cationic species with a tetrahedral geometry, coordination of the metal to one of the dpp fragments takes place, rapidly followed by interaction with the second dpp subunit. The initial process induces complete or nearly complete desolvation of the cation. It is rate limiting and is described by rate laws 3 or 5 for  $\text{Cu}^1$  or  $\text{Ag}^1$ , respectively. Since  $I_t$  is likely to represent an almost completely desolvated state, the rearrangement reaction leading to  $\text{M}(\text{cat-30})$  ( $\text{M} = \text{Cu}^+$ ,  $\text{Ag}^+$ ) is expected to be fast. Since this is not observed under our experimental conditions, we believe that as soon as binding of the cationic species to one of the coordinating subunits has taken place, the other ring rotates rapidly within the first one, leading to the catenate  $\text{M}(\text{cat-30})$ . This type of behavior is reminiscent of allosteric effects found in multi-site coordinating molecular systems.<sup>25,26</sup> In our case, information is rapidly

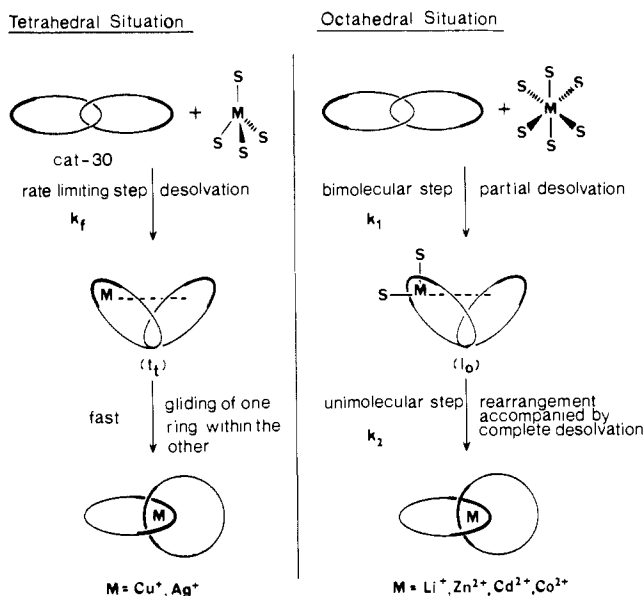
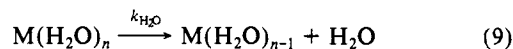


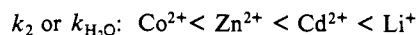
**Figure 5.** Mechanistic hypothesis. The thick lines represent the dpp coordinating sites of cat-30. M and S are respectively the cationic species to be complexed and the solvent. The loose interaction between M and the second dpp fragment in the intermediate complex  $I_t$  or  $I_o$  is symbolized by a dashed line.

transmitted from one dpp to the other, inducing the fast reorganization process  $I_t \rightarrow \text{M}(\text{cat-30})$ . This hypothesis is corroborated by the very fast gliding motions of rings found in multi-catenands related to cat-30, as estimated from <sup>1</sup>H NMR measurements.<sup>27</sup>

On the other hand, the participation of solvent molecules in  $\text{Li}^+$ ,  $\text{Zn}^{2+}$ ,  $\text{Cd}^{2+}$ , and  $\text{Co}^{2+}$  complexation reactions is probably more important. The first step,  $\text{cat-30} \rightarrow I_o$ , is analogous to the bimolecular reaction of cat-30 with the cations that prefer tetrahedral geometry. It involves coordination of the metal center and desolvation. However, this desolvation step is only partial, since the energy required for fully desolvating  $\text{Li}^+$ ,  $\text{Zn}^{2+}$ ,  $\text{Cd}^{2+}$ , or  $\text{Co}^{2+}$  is much higher than that needed for  $\text{Cu}^+$  or  $\text{Ag}^+$ . As a consequence, the intermediate complex  $I_o$  still contains solvent molecules bound to the metal. As for the tetrahedral situation, there probably exists a weak interaction between the cationic species and the second dpp fragment, within the intermediate species  $I_o$ . In order to establish such a loose bond, the organic skeleton may have to undergo geometrical changes, as indicated schematically in Figure 5. The unimolecular step  $I_o \rightarrow \text{M}(\text{cat-30})$  is now noticeably slower since an important kinetic contribution from desolvation is expected. Indeed, the rearrangement process of  $I_o$  to the catenate structure involves the simultaneous release of 2 or more solvent molecules, making this step much slower than the rearrangement of  $I_t$ . The presence of solvent molecules within  $I_o$  is sustained by comparing the  $k_2$  sequence and the dehydration rate constants  $k_{\text{H}_2\text{O}}$  for the series  $\text{Li}^+$ ,  $\text{Zn}^{2+}$ ,  $\text{Cd}^{2+}$ , and  $\text{Co}^{2+}$ .<sup>28</sup>



For both  $k_2$  and  $k_{\text{H}_2\text{O}}$ , the sequence order is the same:



Even if the chemical nature of S in  $I_o$  is not clear ( $\text{CH}_3\text{CN}$  or  $\text{H}_2\text{O}$ ) the trend is likely to be the same for a large variety of solvents, which tends to indicate that the  $k_2$  sequence would parallel that of  $\text{CH}_3\text{CN}$  desolvation. Remarkably, the  $k_2$  sequence parallels that of  $k_{\text{H}_2\text{O}}$  although the kinetics involved do not belong to the same time scale. Indeed, the rearrangement reaction corresponding to  $k_2$  is extremely slow as compared to a dehydration

(24) Irving, H.; Mellor, D. H. *J. Chem. Soc.* **1962**, 5222.

(25) Rebeck, J., Jr. *Acc. Chem. Res.* **1984**, *17*, 258.

(26) Chambron, J.-C.; Sauvage, J. P. *Tetrahedron Lett.* **1986**, *27*, 865.

(27) Edel, A.; Kintzinger, J.-P., unpublished results. Edel, A. Ph.D. Louis Pasteur University, Strasbourg, 1987.

(28) Diebler, H.; Eigen, M.; Illgenfritz, G.; Maas, G.; Winckler, R. *Pure Appl. Chem.* **1969**, *20*, 93.

process (~8 orders of magnitude) or to a classical conformational change. The pathway which leads to the conversion of  $I_0$  to the catenate is very narrow. Fitting together the dpp subunits while unraveling the pentaoxyethylene links from one another and bringing them to the back of the phenanthroline nuclei must be a slow process as long as a solvated metal is present. The compactness of the many intermediate microstates encountered in the course of the transformation of  $I_0$  to  $M(\text{cat-30})$  probably requires simultaneous release of two or more solvent molecules, which drastically slows down the overall complexation reaction.

Until now, all the physical methods used in order to investigate the new class of ligands formed by catenands have shown that those molecules behave as *single chemical species*. The present study illustrates this characteristic property. Kinetically, cat-30 behaves as a *single ligand* and not as two dap subunits. As suggested by the reaction schemes of Figure 5, the dpp fragments do not ignore each other. If cat-30 would act as an ensemble of two separate coordinating molecules, it would probably lead to dinuclear species (each dpp fragment bound to a metal center) at some stage during the complexation reaction. This hypothesis has been checked experimentally by using a large excess of ligand with respect to  $\text{Li}^+$ , whereas the experimental data discussed above have been obtained in a completely inverse situation ( $[\text{ligand}]/[\text{metal cation}] < 0.1$ ). Two steps are still clearly observed although the formation of dimetallic complexes is strongly disfavored.<sup>29</sup>

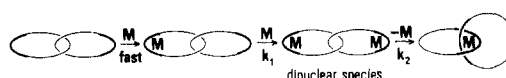
In summary, the present kinetic study points to the unusual properties of catenands with respect to the reaction pathway leading to catenates. In particular, the catenane nature of the ligand cat-30 leads to a surprising two-step reaction for  $\text{Li}^+$ ,  $\text{Zn}^{2+}$ ,  $\text{Cd}^{2+}$ , and  $\text{Co}^{2+}$  complexation. The second step observed is assigned to the gliding motion of one ring within the other, such a process being responsible for the complete rearrangement of the organic skeleton. Owing to the corresponding narrow reaction pathway and to the rigidity and compactness of the final state, this reorganization is remarkably slow.

**Acknowledgment.** We thank the CNRS for its constant financial support.

**Registry No.** m-30, 90030-13-0; dap, 89333-97-1;  $\text{Cu}^+$ , 17493-86-6;  $\text{Ag}^+$ , 14701-21-4;  $\text{Li}^+$ , 17341-24-1;  $\text{Cd}^{2+}$ , 22537-48-0;  $\text{Zn}^{2+}$ , 23713-49-7;  $\text{Co}^{2+}$ , 22541-53-3;  $\text{Cu}(\text{dap})^+$ , 112195-98-9.

(29) Although the "dimetallic hypothesis" represented on the following scheme seems to be highly improbable, it is difficult to totally exclude it at the present stage. We thank Prof. D. W. Margerum for stimulating discussions regarding this problem.

Scheme 1



## Ruthenium(IV)-Oxo Complexes: The Novel Utilization of Tertiary Pnictogen Ligands

Mary E. Marmion and Kenneth J. Takeuchi\*

Contribution from the Department of Chemistry, SUNY at Buffalo, Buffalo, New York 14214.  
Received July 22, 1987

**Abstract:** The novel complexes  $[(\text{bpy})_2(\text{PnR}_3)\text{Ru}^{\text{IV}}(\text{O})](\text{ClO}_4)_2$  (where  $\text{bpy} = 2,2'$ -bipyridine and  $\text{PnR}_3 =$  tertiary phosphine or arsine) have been generated from the analogous ruthenium(II)-aquo species, through electrochemical means or by the addition of two equivalents of cerium(IV). Characterization of the ruthenium(II)-aquo and ruthenium(IV)-oxo complexes was accomplished through UV-vis spectroscopy, IR spectroscopy,  $^{18}\text{O}$  labeling experiments, NMR spectroscopy, cyclic voltammetry, coulometry, and conductivity measurements. These complexes are stable both in the solid state and in various solutions, where the phosphine and arsine ligands do *not* undergo oxidation by the ruthenium(IV)-oxo center. Cyclic voltammetric measurements of the ruthenium(II)-aquo complexes are consistent with the following redox couples:  $\text{Ru}^{\text{IV}}=\text{O}/\text{Ru}^{\text{III}}-\text{OH}/\text{Ru}^{\text{II}}-\text{OH}_2$ , which can be described as two sets of concomitant one-electron, one-proton transfers. The ruthenium(IV)-oxo complexes act as selective oxidation reagents toward organic substrates, where the nature of the pnictogen ligand greatly affects the rate of substrate oxidation. In addition, the use of a pnictogen ligand *cis* to the oxo moiety in these complexes simplifies the mechanism of substrate oxidation relative to other ruthenium-based oxidants. Finally, pnictogen ligands exert unusual effects on the redox chemistry of ruthenium(IV)-oxo complexes, including hydrophobic selectivity and aerobically driven substrate oxidation catalysis.

Ruthenium-oxo/aquo complexes have proven to be very suitable in the design of redox catalysts for a variety of reasons. First, transition metals are useful catalysts in redox reactions since one or more oxidation states are frequently available as a source of or sink for electrons, thus enabling multiple electron transfers to occur. In addition, the substitutionally inert nature of ruthenium<sup>1-3</sup> allows for chemically reversible electron transfer uncomplicated by ligand exchange. Therefore, ruthenium complexes tend to

retain their integrity in solution and are relatively easy to study. Finally, the oxo-aquo ligands provide for rapid proton transfer concomitant with electron transfer permitting the accessibility of several oxidation states via gain or loss of protons.<sup>4,5</sup>

Previously, we reported the first successful syntheses and characterizations of ruthenium(IV)-oxo complexes that contain tertiary phosphine ligands in a position *cis* to the oxo ligand.<sup>6</sup>

(1) Margerum, D. W.; Cayley, G. R.; Weaterburn, D. C.; Pagenkopf, G. K. *Coordination Chemistry*; American Chemical Society: Washington, DC, 1978; ACS Monograph 174, Vol. 2, Chapter 1.

(2) Seddon, E. A.; Seddon, K. R. *The Chemistry of Ruthenium*; Elsevier: New York, 1984.

(3) Griffith, W. P. *The Chemistry of Rarer Platinum Metals*; Interscience: London, 1967.

(4) (a) Takeuchi, K. J.; Samuels, G. J.; Gersten, S. W.; Gilbert, J. A.; Meyer, T. J. *Inorg. Chem.* **1983**, *22*, 1407-1409. (b) Takeuchi, K. J.; Thompson, M. S.; Pipes, D. W.; Meyer, T. J. *Inorg. Chem.* **1984**, *23*, 1845-1851.

(5) (a) Moyer, B. A.; Meyer, T. J. *J. Am. Chem. Soc.* **1978**, *100*, 3601-3603. (b) Moyer, B. A.; Meyer, T. J. *Inorg. Chem.* **1981**, *22*, 436-444.

(6) Marmion, M. E.; Takeuchi, K. J. *J. Am. Chem. Soc.* **1986**, *108*, 510-511.